Parasitology

cambridge.org/par

Targeting HDACs of apicomplexans: structural insights for a better treatment

Caroline de Moraes de Siqueira, Mariana Sayuri Ishikawa Fragoso, Vanessa Rossini Severo, Isis Venturi Biembengut, Sheila Cristina Nardelli and Tatiana de Arruda Campos Brasil de Souza

Instituto Carlos Chagas – Fundação Oswaldo Cruz – Fiocruz/PR, Curitiba, PR, Brazil

Research Article

Cite this article: de Siqueira CdeM, Fragoso MSI, Severo VR, Biembengut IV, Nardelli SC, de Souza TdeACB (2022). Targeting HDACs of apicomplexans: structural insights for a better treatment. *Parasitology* **149**, 956–967. https://doi.org/10.1017/S0031182022000427

Received: 31 October 2021
Revised: 18 March 2022
Accepted: 19 March 2022
First published online: 31 March 2022

Key words:
Apicidin; Apicomplexa; HDAC inhibitor; HDACs; homology modelling; molecular docking

Author for correspondence:
Tatiana de Arruda Campos Brasil de Souza,
E-mail: tatiana.brasil@fiocruz.br

Abstract

Aetiologic agents of diseases such as malaria and toxoplasmosis are found in representatives of the phylum Apicomplexa. Therefore, apicomplexan parasites are known to have a significant impact on public health. Epigenetic factors such as histone acetylation/deacetylation are among the main mechanisms of gene regulation in these parasites. Histone deacetylases (HDACs) have aroused a great deal of interest over the past 20 years for being promising targets in the development of drugs for treating several diseases such as cancer. In addition, they have also been shown to be effective for parasitic diseases. However, little is known about the structure of these proteins, as well as their interactions with specific ligands. In this paper, we modelled 14 HDACs from different apicomplexan parasites and performed molecular docking with 12 ligands analogous to the HDAC inhibitors FR235222 and apicidin, which had previously been tested against *Toxoplasma gondii* and *Plasmodium falciparum*. In this *in silico* study, we were able to gather relevant structural data regarding these proteins as well as insights into protein–ligand interactions for testing and developing drugs for these diseases.

Introduction

The phylum Apicomplexa comprises a large group of protozoan parasites. Many of them, such as *Toxoplasma gondii*, *Plasmodium* sp. and *Cryptosporidium* sp., cause diseases in humans, while others ail domestic animals, as is the case with *Neospora caninum* (Morrison, 2009). These organisms are characterized by the presence of the apical complex, which is a set of structures formed by rhoptries and micronemes responsible for the parasite's active invasion of the host cell (Frénal *et al.*, 2017). Some members of this phylum have another unique organelle, the apicoplast, which has a secondary endosymbiotic origin and is involved in several cellular processes. This organelle is essential to the survival of these parasites and is an excellent target for drug development. Another peculiarity of the phylum is the highly complex life cycles of its representatives, which alternate between different hosts. This life cycle is robustly regulated by gene expression that controls the adaptation and alteration among the parasites' life forms (Frénal *et al.*, 2017).

During this transition, the parasites undergo morphological, biochemical and molecular changes. It is currently known that about 18% of genes are regulated in a stage-specific manner by unknown transcriptional regulators in *Toxoplasma* sp. (Radke *et al.*, 2005). Many apicomplexans lack canonical transcription factors. However, a family known as AP2-like has been linked to the Apetala-2 transcription factor in plants (Balaji, 2005). These factors have been studied extensively in order to investigate whether they play a role in transcriptional regulation (Painter *et al.*, 2011; Iwanaga *et al.*, 2012; Oberstaller *et al.*, 2014; Jeninga *et al.*, 2019; Srivastava *et al.*, 2020). That said, epigenetic regulation has already proven to be efficient in transcriptional regulation. Among all histone modifications, acetylation seems to be the most abundant. In this context, both canonical and histone variants are hyperacetylated, especially at the N-terminal tails. Also, these histones suffer several other modifications (Nardelli *et al.*, 2013). Several modifiers were identified besides deacetylase and acetyltransferases (ToxoDB.org), and acetylation is one of the most abundant.

Histone deacetylases (HDACs) and histone acetyltransferases (HATs) are mainly responsible for histone acetylation/deacetylation complexes (Inoue and Fujimoto, 1969; Seto and Yoshida, 2014; Sepehri *et al.*, 2019). However, they can have other non-histone targets (Seto and Yoshida, 2014; Verdin and Ott, 2015). One of the most well-known functions of these enzymes is their role in transcription. Histone acetylation, promoted by HATs, makes chromatin more open and accessible to transcription machinery, favouring gene transcription. On the other hand, HDACs remove acetylations and render chromatin inaccessible, consequently preventing transcription and silencing genes. Although this is the most well-known function of HDACs, they also play a role in other processes such as DNA repair and replication (Seto and Yoshida, 2014).

HDACs are traditionally divided into four classes according to their domain, their similarity to yeast sequences, cofactors and inhibition of trichostatin A. Classical zinc-dependent HDACs belong to classes I, II and IV. Contrastingly, non-classical domains are categorized

CAMBRIDGE UNIVERSITY PRESS

into class III; they are known as sirtuins and use nicotinamide adenine dinucleotide (NAD)+ as a cofactor.

HDACs have been studied as a target for drugs supporting the treatment of several illnesses, including cancer and degenerative diseases such as Alzheimer's disease; many HDAC inhibitors have been approved by the U.S. Food and Drug Administration thus far (Benedetti *et al*., 2015). In 1996, Darkin-Rattray and colleagues reported the effectiveness of HDAC inhibitors against *Plasmodium* sp. Since their publication, other HDAC inhibitors have been tested (Bougdour *et al*., 2009), and interesting effects have been observed, not only with regards to apicomplexans but for other parasites as well, like the Euglenozoa *Trypanosoma* sp. and *Leishmania* sp., cestodes and the trematode *Schistosoma* sp. (Andrews *et al*., 2012; Chua *et al*., 2017; Guidi *et al*., 2018; Vaca *et al*., 2021). Even so, little is known about the HDACs of apicomplexan species. Thus far, there are no studies focused on thoroughly addressing their structure by employing X-ray crystallography. Moreover, the binding mechanism of these inhibitors in the HDACs' structure is unknown.

Homology modelling is a powerful tool for understanding protein structures that have no solved structure. This approach is based on the principle that proteins with similar amino acid sequences have similar tertiary structures (Chahal *et al*., 2020). Based on the three-dimensional structure model, it is possible to perform several analyses such as docking, screening and drug discovery; it is a useful technique since many ligands can be used in this field of study.

Therefore, we modelled the HDACs from *T. gondii*, *Plasmodium falciparum*, *Cryptosporidium parvum*, *Cyclospora cayetanensis*, *N. caninum* and *Hammondia hammondi* to explore the specificity of inhibitors that are analogous to FR235222 and apicidin on those HDACs. We chose FR235222 and apicidin compounds because they have already been tested on parasites (Darkin-Rattray *et al*., 1996; Mori *et al*., 2003; Bougdour *et al*., 2009) and their analogues were also tested for HDAC inhibition (Colletti *et al*., 2001; Miller *et al*., 2003; Di Micco *et al*., 2008; Terui *et al*., 2008; Ballante *et al*., 2017). To this end, we performed docking followed by structural analysis to give information about the probable mode of binding and to provide relevant information for drug development.

Materials and methods

In silico *modelling*

Table 1 shows 14 Apicomplexan HDACs whose amino acid sequences were obtained from the following databases: Toxodb.org, Plasmodb.org and Cryptodb.org [TgHDAC2 (TGME49_249620); TgHDAC3 (TGME49_227290); TgHDAC4 (TGME49_227790); TGME49_227790; CpHDAC1 (cgd6_80); CpHDAC2 (cgd6_1380); CpHDAC3 (cgd8_480); PfHDAC1 (PF3D7_0925700); CcHDAC1 (cyc_00497); CcHDAC3 (cyc_03294); HhHDAC2 (HHA_249620); HhHDAC3 (HHA_227290); HhHDAC4 (HHA_257790); NcHDAC4 (CEL67040.1)]. These protein sequences were submitted to the HHPRED server to detect homologies and predict structures (Söding *et al*., 2005). A sequence alignment of the target and protein using atomic structure to present the highest homology was used as an input in the Modeller program (Webb and Sali, 2016). All alignments obtained in this study are available at https://drive.google.com/file/d/135QLmSBR4gIu0cxyhQ6nSIyXBrTuMOF/view?usp=sharing. A total of 50 models was generated for each target, and the best models were selected according to their discrete optimized protein energy (DOPE) score. For molecular modelling, ions bound to template structures were removed. The model's quality was also analysed in the ProSA-web (Wiederstein and Sippl, 2007) and Ramachandran plot (https://zlab.umassmed.edu/bu/rama/) servers.

It is also worth mentioning that TgHDAC4 was misannotated in the database, and our group noticed that the TgHDAC4 mRNA was longer than expected. Thereupon, Dr Arnab Pain's group (King Abdullah University of Science and Technology, Saudi Arabia) reanalysed the RNA-seq data and helped us to properly reassemble the gene by including two more exons that had been missing in the first annotation (Ramaprasad *et al*., 2015).

Molecular docking

Molecular docking was performed using Chimera (Pettersen *et al*., 2004) and AutoDocK Vina (Trott and Olson, 2010) programs. The structure of human HDAC2 linked with the HDAC inhibitor suberoylanilide hydroxamic acid (SAHA) was used as the reference (file code: 4LXZ) to set-up the grid box (Supplementary Fig. S1).

Docking simulations were performed with 12 compounds (1: FR235222; 2: CHEMBL 4099599; 3: CHEMBL 2370998; 4: CHEMBL 358276; 5: CHEMBL 472574; 6: CHEMBL 470325; 7: CHEMBL 492600; 8: CHEMBL 488096; 9: CHEMBL451169; 10: CHEMBL 1793810; 11: CHEMBL 1793988; 12: apicidin, 13: panobinostat, 14: chloroquine) (Fig. 1). These compounds were named ligands 1 to 14. The PDB structures of these compounds were downloaded from the ChEMBL database. They were chosen for being analogues of FR235222 (compounds 4, 5, 6, 7 and 8) and apicidin (compounds 2, 3, 9, 10 and 11). In addition, compounds 13 and 14 are hydroxamate-based inhibitors and were chosen based on previous *in vitro* assays indicating their ability to inhibit *Plasmodium* HDACs (Chua *et al*., 2017).

The docking simulations were performed as follows: (1) each HDAC model was checked for missing atoms, bonds and contacts; subsequently, energy minimization was assessed using the molecular modelling toolkit (MMTK) package on Chimera version 1.14 employing the following parameters: Amber ff14SB force field; 100 steepest descent steps, with a steepest descend step size of 0.02 Å; 10 conjugate gradient steps, with a conjugate gradient step size of 0.02 Å. The minimized structure was used as the receptor for docking analysis. (2) AutoDock Tools module was used to generate pdbqt input files. (3) AutoDock Vina algorithm was used to perform a docking with the selected ligands. The docking simulation was then run at an exhaustiveness = 8. The docking results were evaluated using the lowest binding affinity score (kcal mol^{-1}) predicted by the built-in scoring function of the AutoDock Vina module.

The feasibility and robustness of our interactions are strengthened by comparing the docking results of human HDAC2 interaction with SAHA and the corresponding crystallographic structure was deposited under the code 4LXZ. Both ligand structures presented a root-mean-square deviation (RMSD) of 1.72 Å, indicating both docking and experimental structures are very similar.

Structural analysis

All structural analyses and creation of images were carried out with PyMOL (the PyMOL Molecular Graphics System, version 2.4 Schrödinger, LLC) and Chimera version 1.14 (Pettersen *et al*., 2004). Interactions between protein and ligands were analysed using PDBePISA (proteins, interfaces, structures and assemblies PISA service) at the European Bioinformatics Institute (http://www.ebi.ac.uk/pdbe/prot_int/pistart.html) and/or using PDBsum (Laskowski *et al*., 2018).

Molecular dynamics

Molecular dynamics simulations were performed for a period of 30 ns for CpHDAC1, CpHDAC2, PfHDAC1 and TgHDAC3

https://doi.org/10.1017/S0031182022000427 Published online by Cambridge University Press

Table 1. Proteins selected for analysis

Organism	Protein	Gene ID	Template	PDB ID	Sequence identity (%)
Toxoplasma gondii	HDAC2	TGME49_249620-t26_1	HsHDAC1	5ICN_B	56
	HDAC3	TGME49_227290-t26_1	HsHDAC1	4BKX_B	65
	HDAC4	TGME49_257790-t26_1	BalHDAH	5G17_A	34
	HDAC5	TGME49_202230-t26_1	DrHDAC10	5TD7_A	45
Plasmodium falciparum	HDAC1	PF3D7_0925700.1	HsHDAC1	4BKX_B	61
Cryptosporidium parvum	HDAC1	cgd6_80	HsHDAC1	4BKX_B	65
	HDAC2	cgd6_1380	HsHDAC1	4BKX_B	58
	HDAC3	cgd8_480 XP_625509	PpHDAC	5JI5_A	35
Cyclospora cayetanensis	HDAC 0.18956 (HDAC1)	cyc_00497	HsHDAC1	4BKX_B	44
	HDAC3	cyc_03294	HsHDAC1	4BKX_B	65
Neospora caninum	HDAC4	CEL67040.1	SpCLR3	5IKK	30
Hammondia hammondi	HDAC2	HHA_249620	HsHDAC1	5ICN_B	65
	HDAC3	HHA_227290	HsHDAC1	4BKX_B	65
	HDAC4	HHA_257790	HsHDAC3	4A69	31

Proteins used in this study, their gene ID and the corresponding templates used to generate homology models.

models. GROMACS 2020.4 (Abraham *et al.*, 2015) and CHARMM36m (version jul-2021) (Huang *et al.*, 2017) force field were used to prepare topologies and coordination files. Protonation states were assigned using H++ server version 4.0 (Anandakrishnan *et al.*, 2012) considering the pH 7.4. The models were immersed in a dodecahedron simulative box, 15 Å away from the protein surface, filled with transferable intermolecular potential with 3 points (TIP3P) (Jorgensen *et al.*, 1983) explicit solvent molecules and rendered electroneutral by the introduction of sodium counterions.

A first round of minimization using the steepest descent algorithm (Haug *et al.*, 1976) was performed using several steps where maximum force <1000.0 kJ mol^{-1} nm^{-1} in order to regularize the structures. Optimization and relaxation of solvent and ions were performed in two steps (isothermal–isochoric ensemble and isothermal–isobaric ensemble) by simulating the system at a temperature of 310 K and pressure of 1 bar. The simulation was carried out under periodic boundary conditions with a time step of 2.0 fs at a constant temperature of 310 K using the modified Berendsen thermostat (V-rescale algorithm) (Bussi *et al.*, 2007). Electrostatic interactions were treated using the particle-mesh Ewald algorithm (Essmann *et al.*, 1995). The resultant trajectory, RMSDs and root-mean-square fluctuations were processed using the GROMACS 2020.4 package.

Results

Homology models

We generated structural models of 14 apicomplexan HDACs by homology modelling (Table 1, Fig. 2) since all proteins showed identity with their respective templates above 30% (Sánchez and Sali, 1997). The low sequence homology impaired the modelling of other HDACs such as TgHDAC1, PfHDAC2 and PfHDAC3. These proteins have a long unique sequence of amino acids which could generate unreliable structural data, so we decided to remove them from the analysis. Initially, we observed that almost all the proteins had insertions (mainly C-terminal) with no fold similarity to other known structures. Therefore, the function of those insertions is unknown and should be further investigated through experimental structural approaches such as X-ray crystallography and nuclear magnetic resonance (NMR) for more accuracy in structure determination. In this study, we focused on HDAC domains showing structural homology. Table 2 displays the non-modelled C-terminal regions of all of the proteins (insertions with no previous structure). The quality assessment of the best models (selected based on DOPE score) analysed by ProSA-web and Ramachandran plot servers showed that at least 91% of the residues fell within the most favourable regions (Table 3) (Anderson *et al.*, 2005). The CpHDAC2 and TgHDAC3 were the best models, with more than 99% of the residues in favourable regions of the Ramachandran plot. CpHDAC1 has shown the best *Z* score value (−9.31) (Wiederstein and Sippl, 2007). The *Z* score indicates a more favourable model according to X-ray crystallography and NMR experimental data present in the PDB (Wiederstein and Sippl, 2007). This approach is used to validate a model and identify an erroneous structure. Protein misfolding models have a high energy and *Z* score; the lower the *Z* score, the higher the probability the model is correct (Sippl, 1993). In summary, these analyses show that all the models in this study are of good quality.

Docking

We analysed the binding potential of 12 compounds against 14 proteins. The molecules used for molecular docking were chosen due to their known activity against parasites such as apicidin (Darkin-Rattray *et al.*, 1996) and FR235222 (Mori *et al.*, 2003; Bougdour *et al.*, 2009). Other compounds analogue to these were also selected to evaluate the affinity and chemical properties that can affect affinity

Table 4 describes the binding energy (in kcal mol^{-1}) regarding the best placement of 12 compounds against each protein. TgHDAC5 and HhHDAC2 were the proteins containing more ligands with potential binding affinity with values above −7.5 kcal mol^{-1}. Of all of the HDACs, TgHDAC5 and HhHDAC2 were the proteins that had more interactions below −7.5. Our analysis demonstrated that ligands 4, 5 and 9 have the potential to inhibit most apicomplexan HDACs.

Among the three compounds, ligand 9 was the one that interacted with the largest number of species. Also, ligand 9 was unique to 4 of the 6 apicomplexans analysed. Moreover, no

https://doi.org/10.1017/S0031182022000427 Published online by Cambridge University Press

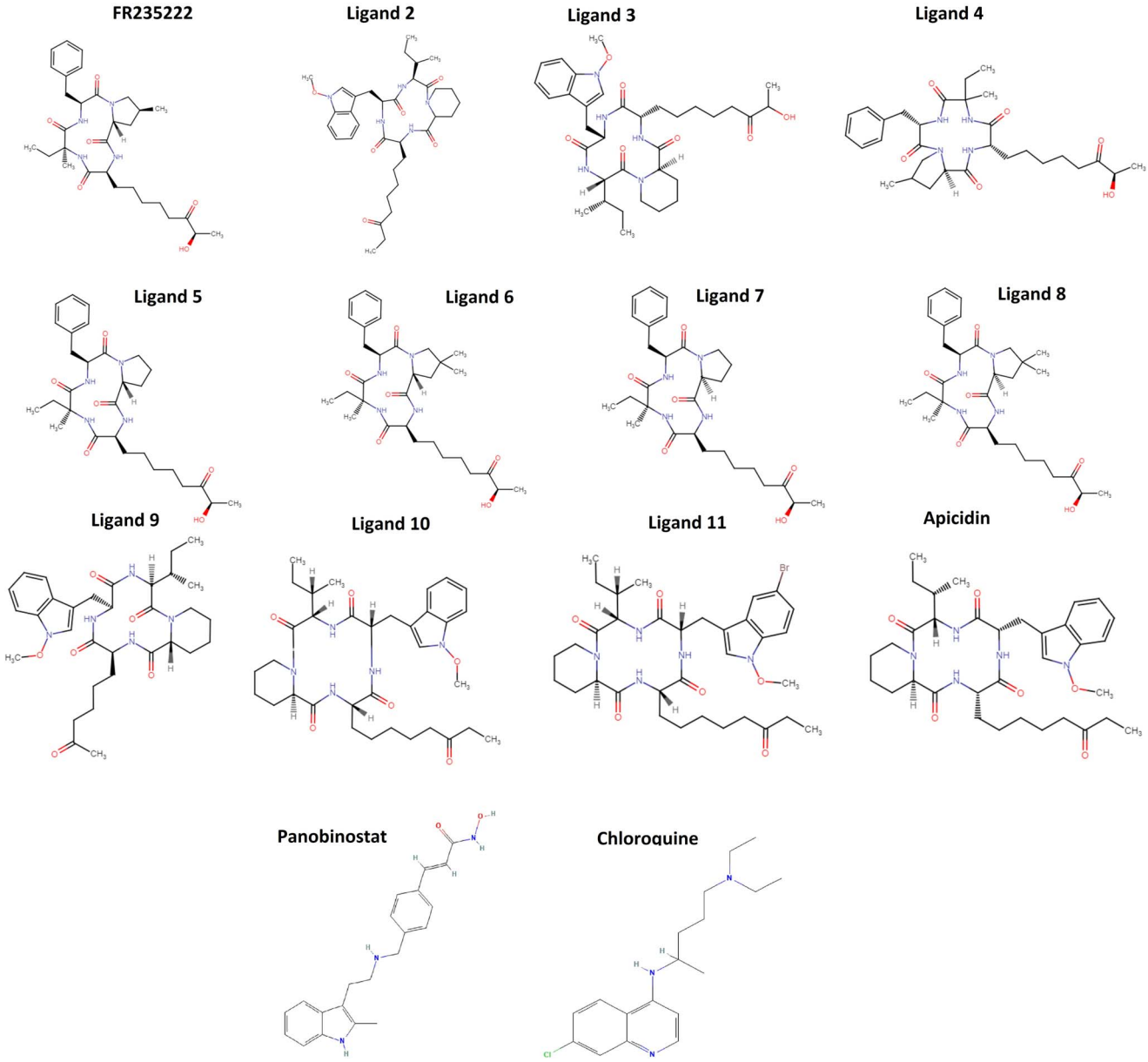

Fig. 1. Ligand structures used in this study. Ligand 1 (FR235222), ligand 2 (CHEMBL4099599), ligand 3 (CHEMBL2370998), ligand 4 (CHEMBL358276), ligand 5 (CHEMBL472574), ligand 6 (CHEMBL470325), ligand 7 (CHEMBL492600), ligand 8 (CHEMBL488096), ligand 9 (CHEMBL451169), ligand 10 (CHEMBL179381), ligand 11 (CHEMBL1793988) and ligand 12 (apicidin); ligand 13 (panobinostat) and ligand 14 (chloroquine). Ligand 7 is the *trans*-form of ligand 5, and ligand 6 is the *cis*-form of ligand 8.

studied compounds displayed a strong affinity to *C. cayetanensis* and *N. caninum* HDACs as observed through their binding affinity values above -7.0 kcal mol^{-1}.

Ligand 4 is analogous to FR235222 and, according to the ChEMBL database, it exhibits inhibitory activity against HT-29 and Jurkat human tumour cells at concentrations of 0.025 and 0.019 nM, respectively (Miller *et al.*, 2003). We emphasize the strongest interaction of this ligand with TgHDAC3. Although this protein is known to be inhibited by the FR235222 compound (Bougdour *et al.*, 2009), the interaction with ligand 4 appears to be stronger than what occurs with the original FR235222 compound.

Ligand 5 is also an analogue of FR235222, synthesized to be a simplification of the original compound. Di Micco *et al.* (2008) observed that this compound presented a better pharmacological profile, better results in inhibition *in vitro* tests, and therefore a better specificity compared to FR235222, which is in line with our findings. Furthermore, this compound showed strong interactions with several HDACs addressed in our study. The strongest interaction was with TgHDAC5, indicating that ligands 4 and 5 have the broadest inhibiting capacity among the apicomplexan HDACs.

Compound 9 is analogous to apicidin, with about 87% similarity. This compound was described in 2008 by Terui and collaborators through the fermentation of *Nonomuraea* sp. TA-0426 (Terui *et al.*, 2008). Besides an HDAC inhibitor, compound 9 is also a glycine transporter type I (GlyT1) inhibitor, a promising target for an antipsychotic treatment (Terui *et al.*, 2008).

We also wish to highlight the interaction of ligand 3 with CcHDAC1, which appears to be specific. The half-maximal inhibitory concentration (IC_{50}) of this compound has already been determined for *P. falciparum* (0.034 nM) and *C. parvum* (4 nM) (Miller *et al.*, 2003). This compound was also tested against HeLa cells and effectively inhibited HDACs in this tumour lineage (Miller *et al.*, 2003). Ligand 6 was synthesized as a variation of FR235222, and we observed that for CcHDAC1 and CpHDAC3,

https://doi.org/10.1017/S0031182022000427 Published online by Cambridge University Press

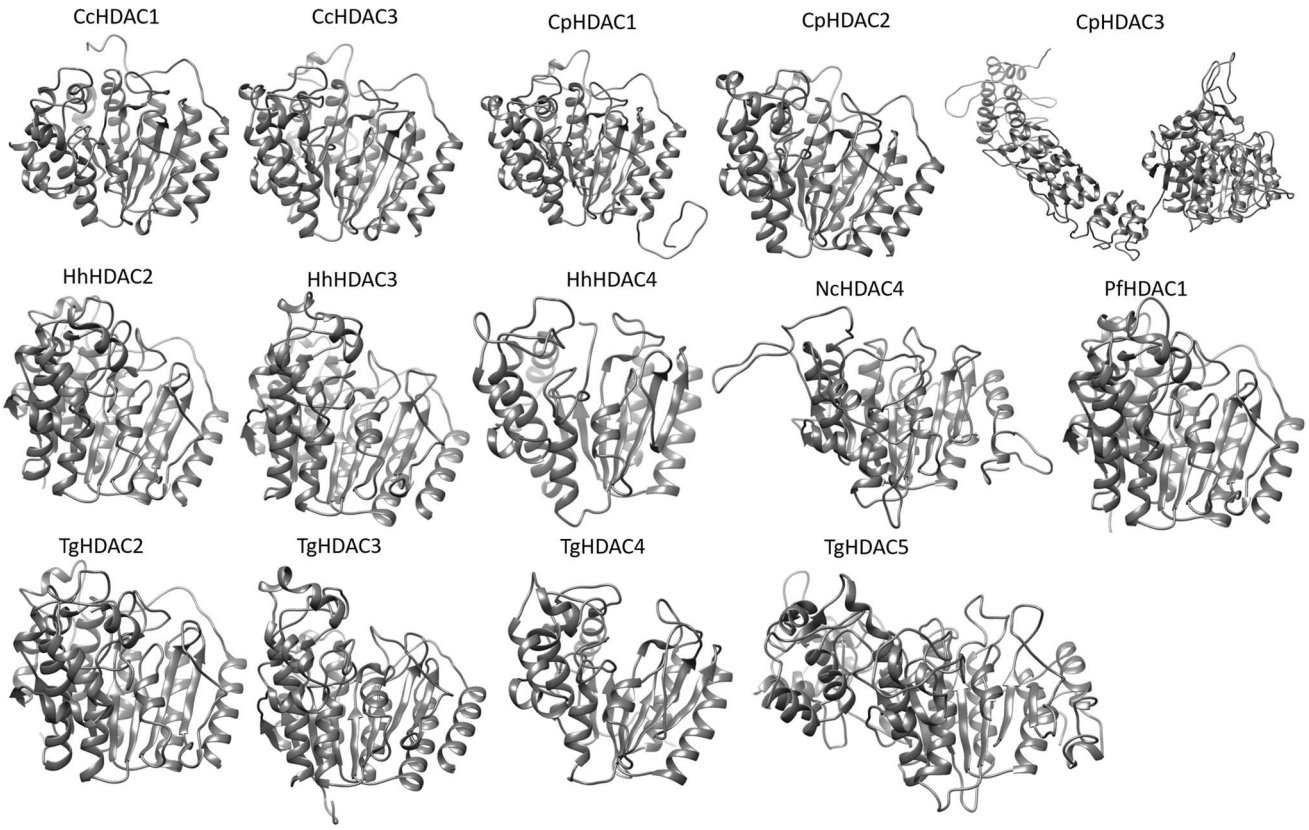

Fig. 2. Tridimensional models of apicomplexan HDACs.

Table 2. Deleted regions

Protein	Protein length	Non-aligned region
CcHDAC1	543	65–151; 383–451; 489–543
CcHDAC3	742	1–71; 421–742
CpHDAC1	444	390–444
CpHDAC2	432	390–432
CpHDAC3	973	1–22; 399–409; 844–973
HhHDAC2	623	76–270; 560–623
HhHDAC3	742	1–17; 375–451
HhHDAC4	1143	1–661; 869–1023
NcHDAC4	1158	1–649; 1003–1158
PfHDAC1	449	372–449
TgHDAC2	624	80–275; 561–624
TgHDAC3	451	374–451
TgHDAC4	1152	1–709; 789–1152
TgHDAC5	1452	1–61; 115–217; 246–373; 428–651; 741–797; 933–1041; 1075–1153; 1299–1452

Many apicomplexan HDACs have insertions that cannot be modelled because they are not homologous to the template protein; therefore, they were not considered in our study.

Table 3. Analysis of the quality of the models

Protein	Ramachandran (%)	*Z* score	DOPE score
CcHDAC1	98.94	−6.71	−3188.68
CcHDAC3	98.41	−7	−8742.20
CpHDAC1	98.51	−9.31	−2024.82
CpHDAC2	99.68	−7.91	−2098.28
CpHDAC3	94.89	−7.03	−6588.59
HhHDAC2	98.72	−7.68	−5870.77
HhHDAC3	98.41	−8.69	−8742.20
HhHDAC4	95.29	−4.95	−2044.37
NcHDAC4	95.72	−4.48	−2518.22
PfHDAC1	97.54	−8.78	−2201.64
TgHDAC2	98.73	−8.34	−3323.08
TgHDAC3	99.07	−8.62	−2143.56
TgHDAC4	95.91	−4.86	−2098.72
TgHDAC5	91.18	−3.5	−12 149.73

Protein models were selected based on the best DOPE scores and were analysed by Ramachandran plot and *Z* score to validate the model.

ligand 6 seems to be stronger and poses a more specific interaction than the original compound. Interestingly, ligand 8, which is the *trans*-form of ligand 6, was more specific in the interaction with HhHDAC4, indicating an important difference between the conformation of the ligand and the strength of interaction with the protein. In addition to HhHDAC4, TgHDAC4 and CcHDAC3 are also potential targets of compound 8.

Compound 11 is among those that least interacted with apicomplexan HDACs. This apicidin analogue had already been tested with *P. falciparum* and *Eimeria tenella*, presenting negligible inhibitory potential. The IC_{50} values were 782 718.90 and 711 562.64 nM, respectively, much higher than what was the case for the original compound (Colletti *et al.*, 2001). The authors indicated that indole modification of the original compound by 5-bromoindole reduces the biological activity and specificity of

https://doi.org/10.1017/S0031182022000427 Published online by Cambridge University Press

Table 4. Ligand binding energy against apicomplexan HDACs

	Ligand													
Protein	1	2	3	4	5	6	7	8	9	10	11	12	13	14
	FR235222	CHEMBL 4099599	CHEMBL 2370998	CHEMBL 358276	CHEMBL 472574	CHEMBL 470325	CHEMBL 492600	CHEMBL 488096	CHEMBL 451169	CHEMBL 1793810	CHEMBL 1793988	Apicidin	Panobinostat	Chloroquine
CcHDAC1	−7.1	n/a	−7.0	−7.1	−7.2	−7.6	−6.1	−6.9	−4.6	−7.4	−6.7	−6.6	−7.9	−5.5
CcHDAC3	−7.2	−6.9	−7.5	−7.4	−6.5	−6.5	−7.1	−7.4	−6.9	−6.7	−7.3	−6.9	−5.8	−5.1
CpHDAC1	−7.2	−7.3	−7.0	−7.5	−7.5	−6.5	−7.5	−6.6	−7.7	−7.9	−7.0	−7.6	−6.3	−3.7
CpHDAC2	−7.1	−8.2	−7.0	−6.7	−7.5	−7.2	−6.7	−6.3	−7.9	−6.9	−8.3	−8.2	−8.0	−5.9
CpHDAC3	−6.6	−6.3	−7.0	−5.5	−7.0	−7.4	−6.0	−6.8	−6.7	−6.5	−2.6	−7.0	−6.9	−5.6
HhHDAC2	−5.6	−7.7	−8.1	−8.2	−8.0	−8.4	−6.3	−6.6	−8.0	−6.9	−7.8	−8.0	−7.6	−5.5
HhHDAC3	−7.5	−7.1	−6.6	−7.5	−7.2	−7.4	−7.3	−7.3	−7.0	−6.8	−7.1	−6.3	−7.7	−5.3
HhHDAC4	−5.8	−7.4	−6.5	−7.0	−5.0	−5.5	−6.2	−7.5	−6.0	−7.0	−7.4	−7.3	−6.1	−6.3
NcHDAC4	−6.4	−6.9	−6.2	−7.0	−6.7	−6.8	−6.3	−6.4	−7.2	−6.7	−6.6	−7.2	−8.0	−7.1
PfHDAC1	−6.5	−6.8	−6.5	−7.0	−7.4	−7.5	−7.2	−7.5	−7.5	−7.3	−7.0	−7.5	−6.6	−5.9
TgHDAC2	−7.5	−6.8	−8.2	−7.5	−7.5	−7.8	−6.8	−6.7	−8.1	−7.5	−6.9	−6.9	−8.4	−5.5
TgHDAC3	−7.0	−7.1	−6.6	−7.7	−6.9	−7.0	−7.2	−6.4	−6.5	−6.4	−6.3	−7.1	−7.8	−5.6
TgHDAC4	−8.1	−7.6	−6.7	−7.9	−7.7	−6.4	−6/9	−7.8	−7.0	−7.4	−6.8	−6.9	−8.0	−5.7
TgHDAC5	−8.1	−7.4	−8.2	−8.7	−8.9	−8.6	−8.0	−7.8	−8.1	−8.7	−7.7	−7.6	−7.1	−6.7

This table shows the scores for molecular docking binding energy. The molecular docking was performed with 14 ligands against 14 apicomplexan HDACs.

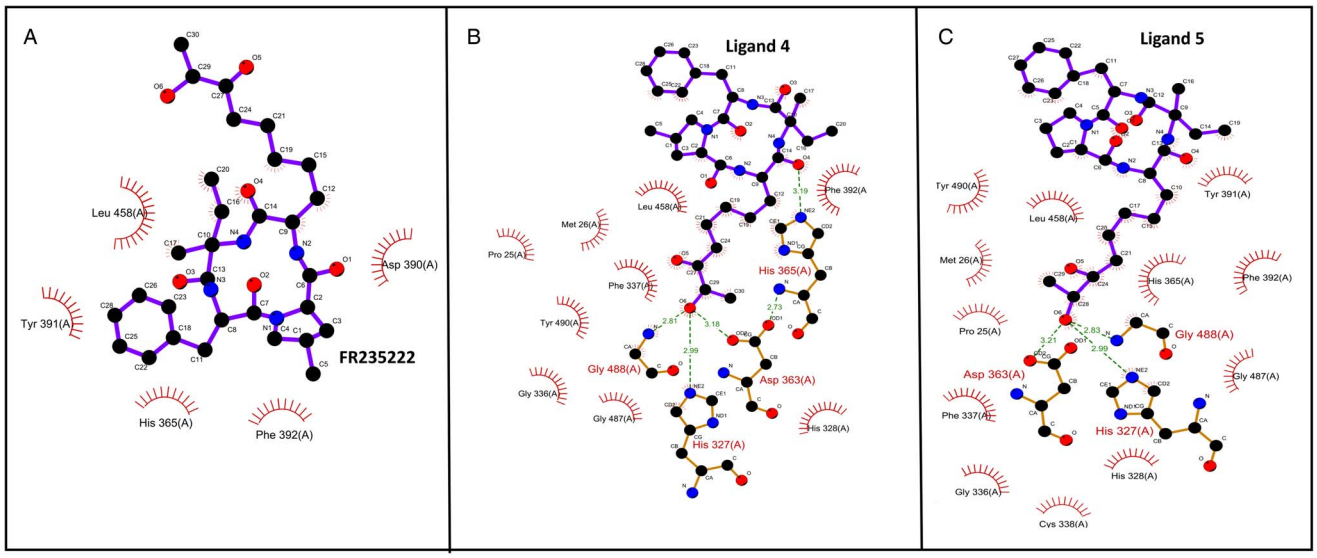

Fig. 3. Interaction map with HhHDAC2. Bidimensional map of the interaction between HhHDAC2 and ligands (A) FR235222, (B) 4 and (C) 5, showing van der Walls interactions (⌒) and hydrogen bonds (▬ ▬ ▬).

the compound in relation to the original, which is supported by our study, where apicidin also showed better results.

Regarding hydroxamate-based inhibitors, panobinostat seemed to have more affinity to tested HDACs with greatest scores for TgHDAC2, TgHDAC4 CpHDAC2, NcHDAC4 and CcHDAC1. Chloroquine theoretical affinity was observed mainly for NcHDAC4.

Molecular dynamics analysis

After 30 ns of simulation, the low RMSD variation indicates the convergence of simulation (Supplementary Fig. S2A). The ligand binding sites (Supplementary Fig. 2B–G) do not present high flexibility (RMSD values of about 0.3 nm). Most flexibility (RMSD values of 0.4 nm) might reside upon loops comprised of residues 16–27 (of CPHDAC1) and 198–205 (of PfHDAC1). The low values of RMSD indicate that conformational flexibility of the binding sites should not substantially alter the results of molecular docking.

Structural analysis of interactions

HhHDAC2 is a class I HDAC that interacts with the FR235222 compound through van der Waals interactions (Fig. 3A). The interaction of HhHDAC2 with ligands 4 and 5 is greater due to the hydrogen bonds (Fig. 3B and C, Table 4). Both compounds interact with D363 and H327 (HhHDAC2 numbering). The difference between the interaction of compounds with this HDAC relies on ligand 4 interactions with H365 and ligand 5 interactions with G488 (Fig. 3B and C). The contribution of interactions between ligand 4 and H327 results in more energy binding compared with ligand 5 (Fig. 3B and C, Table 4).

Regarding ThHDAC5, its interaction with FR235222 is potentially more robust than with HhHDAC2. While HhHDAC2 only formed van der Waals interactions, TgHDAC5 formed hydrogen bond interactions with H638, D363, D898, R409 and G943 (TgHDAC5 numbering). An exchange in the interaction of G943 by R574 was observed with ligand 4. The greater number of van der Walls interactions with ligand 5 might explain its slightly higher potential binding affinity for TgHDAC5.

The ThHDAC5–apicidin interaction includes hydrogen bonds with R574 and G943 (ThHDAC5 numbering). We observed that the substitution of R574 by R409 and the addition of G943 to the ligand–ThHDAC5 interface contribute to a greater potential affinity with ligand 9 than with apicidin (Fig. 4). Therefore, we conclude that the potential residues for inhibition are: D363 (HhHDAC2) and R409, D898, H638 (TgHDAC5). R409 seems to be a critical residue in these potential interactions.

In CcHDAC1 interaction with FR235222 and its analogues, the binding pattern seemed completely different. FR235222 interacts through hydrogen bonds with F268, H266 and G265 (Fig. 5A, CcHDAC1 numbering). On the other hand, ligand 6 interacts with E248, K207 and N276, which appears to result in a stronger interaction (Fig. 5B, Table 4). Notably, the improvement in the binding of CcHDAC1 to ligand 3 arises from the hydrogen bonds with H241 and G14 when compared to the original apicidin compound, which forms only van der Waals interactions (Fig. 5C and D).

An interaction that caught our attention was the one between HhHDAC4 and ligand 8, as this is the *trans*-form of ligand 6 and proved to be much more relevant for inhibiting this protein as well as for other class IV HDACs. In this protein, ligand 6 interacts with residues Y13, G11 and K119 (Fig. 6A). Of these residues, only K119 remained in the interaction map with ligand 8, which also forms three hydrogen bonds with this residue. The interactions with I70, K69 and L72 also appear to be important (Fig. 6B).

Structural comparison among human and apicomplexan HDACs

Superposing of 14 modelled apicomplexan HDACs and human HDAC crystallographic structures (HDAC 2 PDB 4LXZ, HDAC 1 PDB 4BKX, HDAC 3 PDB 4A69, HDAC 8 PDB 5FCW) showed that ligand binding site is very conserved among HDACs. Human HDAC regions 89–97 (HDAC2 numbering) are not conserved in apicomplexan HDACs (Fig. 7A). Among apicomplexans, the ligand binding site of NcHDAC4 diverge more from human HDACs (Fig. 7B).

Discussion

Apicomplexa is a large phylum comprising more than 5000 species, with many non-pathogenic organisms. However, several species pose a risk to public health, such as *T. gondii*,

https://doi.org/10.1017/S0031182022000427 Published online by Cambridge University Press

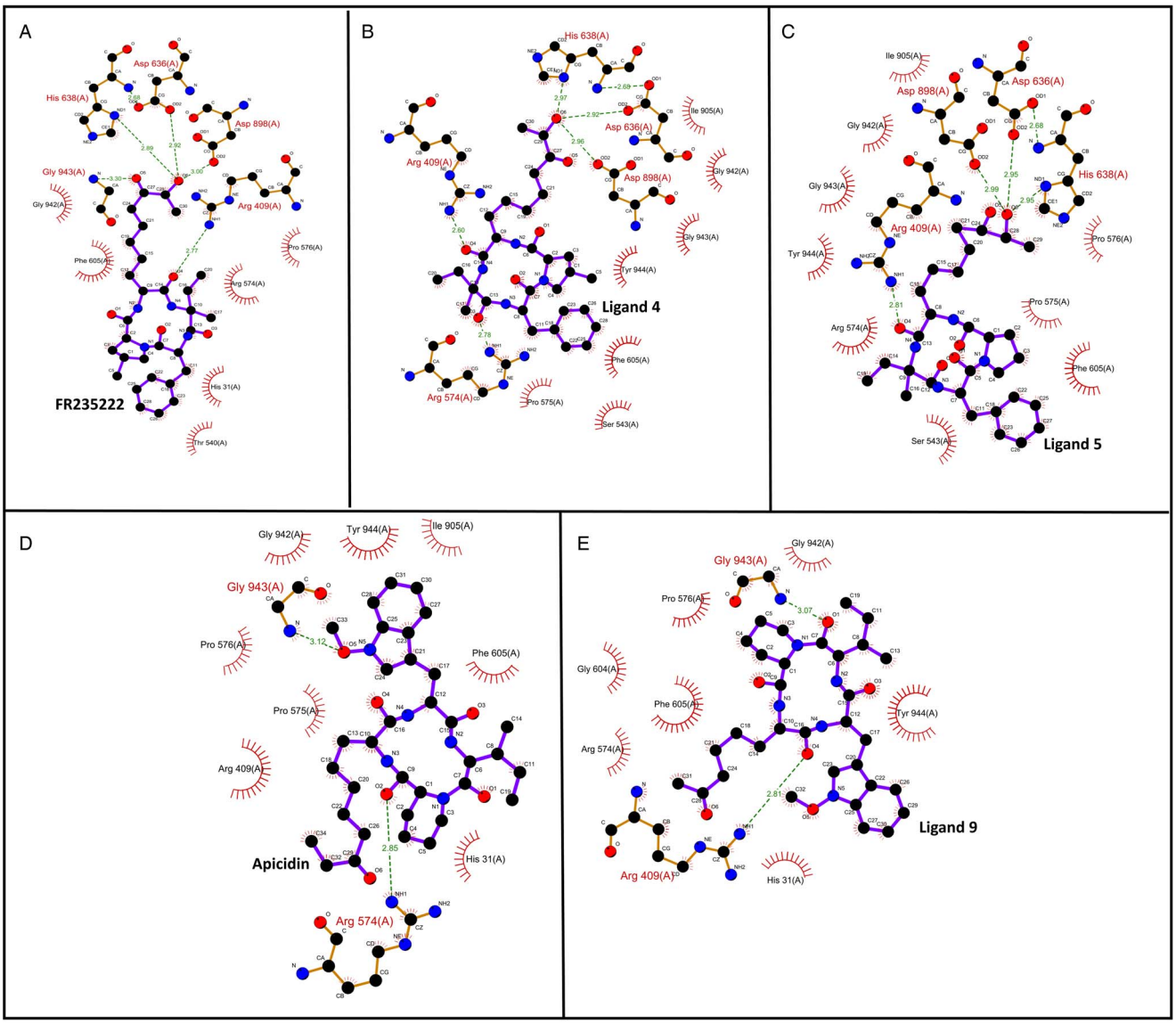

Fig. 4. Interaction map with TgHDAC5. Bidimensional map of interactions between TgHDAC5 and ligands (A) FR235222, (B) 4, (C) 5, (D) apicidin and (E) 9 showing van der Walls interactions (⌒) and hydrogen bonds (- - -).

Plasmodium sp. and *Cryptosporidium* sp., which cause toxoplasmosis, malaria and cryptosporidiosis, respectively. Although well known, these diseases are still neglected due to a lack of effective treatment. In the case of toxoplasmosis, there has been no development of new drugs for over 60 years. Moreover, the commonly used drugs are ineffective in the chronic phase of the disease and cause many side-effects, leading many patients to abandon their treatment (Dunay *et al.*, 2018). On the other hand, malaria presents a high rate of drug resistance, which should prompt more efforts to develop a more effective treatment (WHO Guidelines Approved by the Guidelines Review Committee, 2015).

Inhibitors such as trichostatin A, apicidin and FR235222 have already been tested on some parasites with promising results (Darkin-Rattray *et al.*, 1996; Bougdour *et al.*, 2009; Chua *et al.*, 2017). However, little is known regarding apicomplexan HDACs; thus far, a few articles have been published concerning their structure, and most of them focus on *P. falciparum* HDAC1, which we also address in this study (Melesina *et al.*, 2015; Kumar *et al.*, 2018). PfHDAC1 is expressed in the nucleus of gametocytes in mature blood stages, and its inhibition leads to a global transcriptional dysregulation. Consequently, PfHDAC1 is considered to be a good target for inhibitors (Joshi *et al.*, 1999; Chaal *et al.*, 2010).

This study brings new and important structural data regarding several HDACs. We performed homology modelling of 14 HDACs from 6 apicomplexan parasites. However, this method presents limitations since it depends on homology similarity greater than 30%. Therefore, we were unable to model some of these proteins' regions since they have many insertions with unknown function and structure. The *Saccharomyces cerevisiae* HDACs have a C-terminal coiled-coil domain that functions as a scaffold for the HDAC complex, an evidence that the insertion regions may play a similar role in the Apicomplexa (Lee *et al.*, 2021). We suggest more *in vitro* studies on these proteins should be conducted.

In addition to generating models of HDAC proteins, we also carried out molecular docking with 12 HDAC inhibitors, having FR235222 and apicidin as the positive controls along with 10 other analogous compounds obtained through the ChEMBL database. The validation and analysis of the dockings was carried out, and satisfactory models were obtained as a result.

Some inhibitors tested here have not yet been tested on parasites before, and the docking results form a basis as a guide for

https://doi.org/10.1017/S0031182022000427 Published online by Cambridge University Press

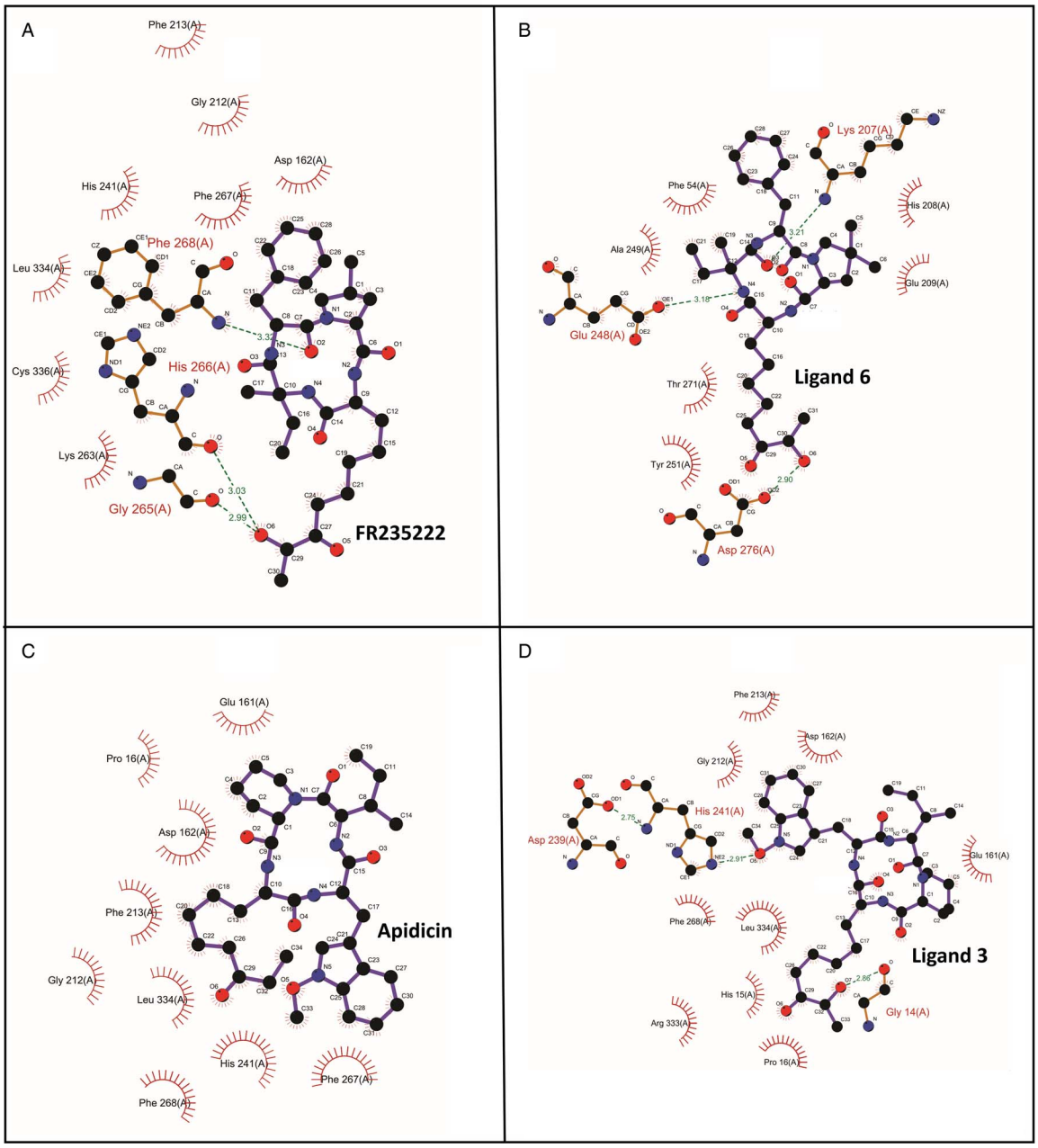

Fig. 5. Interaction map with CcHDAC1. Bidimensional map of interactions between CcHDAC1 and ligands (A) FR235222, (B) 6, (C) apicidin and (D) 3 showing van der Walls interactions (⌒) and hydrogen bonds (▬ ▬ ▬).

future studies. Bougdour *et al.* (2009) demonstrated the activity of FR235222 on *T. gondii* HDAC3, with specific inhibition and increased expression of bradyzoite genes. The authors also detected hyperacetylation of histone H4 in promoter regions.

Ligands 4 and 5, analogous to FR235222, were synthesized to be simpler and more efficient compounds compared to the original compound (Di Micco *et al.*, 2008). These compounds showed good results in tumour cells such as HT-29 and Jurkat at a nanomolar scale. Based on the docking scores of the present study, we recommend that their effectiveness against parasites should be tested. This is particularly valid for *T. gondii*, for which Di Micco *et al.* (2008) achieved promising results in all docked HDACs, especially TgHDAC5.

Bougdour *et al.* (2009) demonstrated the crucial role of the conserved and Apicomplexa HDAC-specific residue TgHDAC3 T99 in the inhibitory activity of FR235222. We observed that TgHDAC3 might be able to bind not only to this catalytic site with a theoretical affinity of −7.1 kcal mol^{-1}, but also to the region that comprised residues 64–67, 165–168 and 187–192 with similar affinity.

Our interaction analysis showed that in some apicomplexans, such as HhHDAC2, the compound FR235222 interacted only through weak bonds, such as van der Waals. Ligands 4 and 5 interact through stronger hydrogen bonds. Furthermore, we verify that targeting R574 (as observed in TgHDAC5–ligand 4) instead of G943 (as observed in HhHDAC2–ligand 4) is important for increasing affinity. Additionally, the ligand proximity between TgHDAC5 and R409 seems to be important for improving the compound affinity.

Apicidin was the first HDAC inhibitor tested on *P. falciparum* and has been proven to be an effective drug both *in vitro* and *in vivo* when tested on mice (Darkin-Rattray *et al.*, 1996). Since then, many analogues have been developed. In this study, among apicidin analogues, ligand 9 showed the best results. This ligand is an inhibitor of GlyT1 and a target for an antipsychotic treatment (Terui *et al.*, 2008). We observed that the difference between

https://doi.org/10.1017/S0031182022000427 Published online by Cambridge University Press

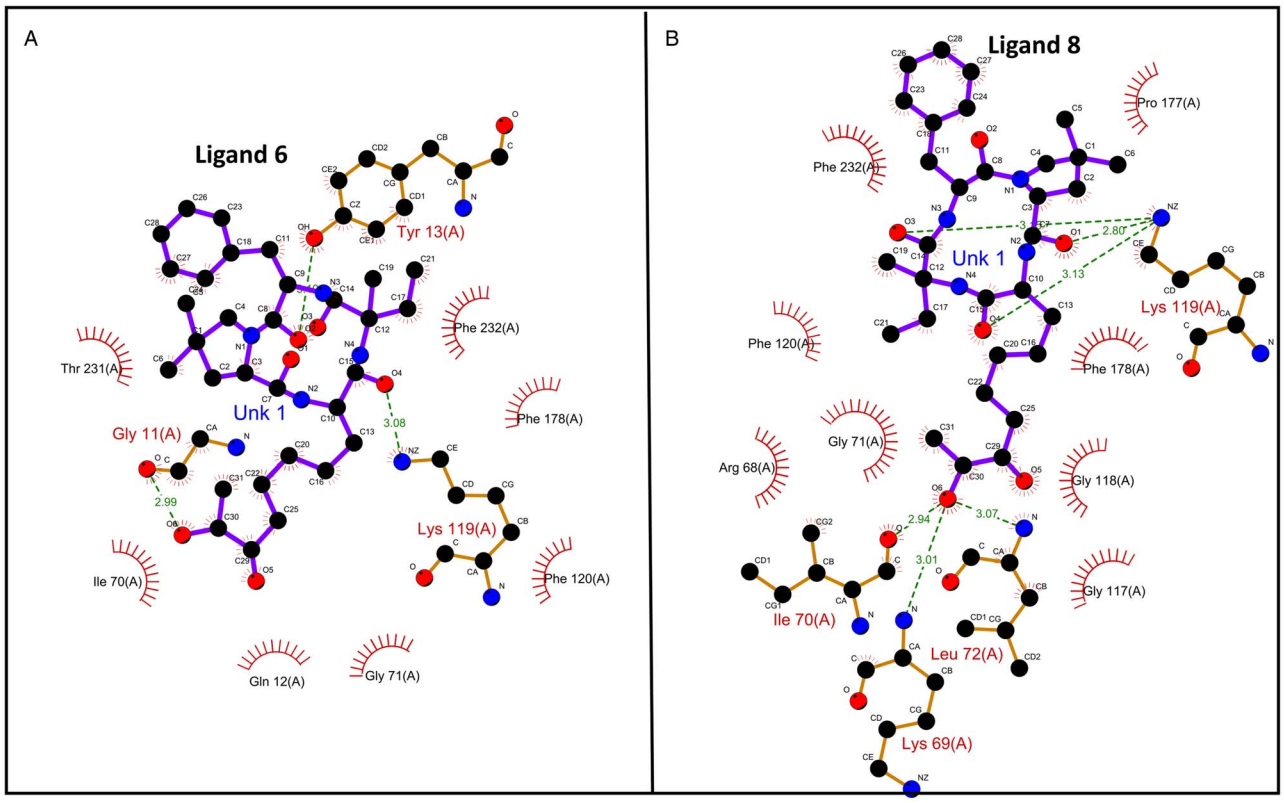

Fig. 6. Interaction map with HhHDAC4. Bidimensional map of the interactions between HhHDAC4 and ligands (A) 6 and (B) 8 showing van der Walls interactions (⌒) and hydrogen bonds (▬ ▬ ▬).

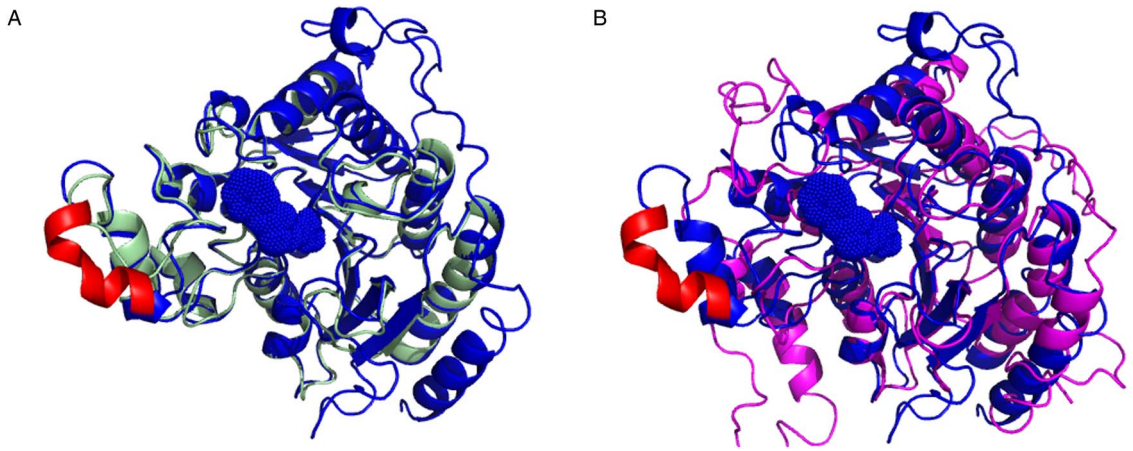

Fig. 7. Similarity among apicomplexan and human HDACs. (A) Superposing of human HDAC2 (PDB 4LX2, blue) and HhHDAC4 (green) representing the conserved fold among HDACs and highlighting the divergent helix in human HDACs (red). (B) Superposing of human HDAC2 (PDB 4LX2, blue) and NcHDAC4 (magenta). Ligand binding site is shown as blue dots.

the binding of ligand 9 and apicidin resides in the replacement of the interaction with R574 by R409; in addition to this, both interactions are closer in ligand 9.

Ligand 3, an apicidin analogue, enhances potential binding by including several hydrogen bonds with CcHDAC1 that were not observed in apicidin–CcHDAC1 interaction and therefore contributed for better docking scores. Ligand 3 had already been tested in *P. falciparum* and *C. parvum*, and its IC_{50} was 0.022 ng mL^{-1} and 4 nM, respectively (Miller *et al.*, 2003). However, this compound appears to be even more specific to *C. cayetanensis* as well as ligand 6, which also proved to be highly specific to CcHDAC1.

The binding of hydroxamate-based inhibitors to PfHDACs was previously tested *in vitro*, with panobinostat and chloroquine presenting IC_{50} of 4 and 10 nm, respectively, the best values against the tested inhibitors (Chua *et al.*, 2017). Our docking results corroborate with a stronger affinity to panobinostat than chloroquine. Also, the affinity of panobinostat to TgHDAC2, TgHDAC4 CpHDAC2, NcHDAC4 and CcHDAC1 might be stronger than that observed for *Plasmodium* HDAC (Chua *et al.*, 2017). Also, chloroquine affinity to NcHDAC4 might be higher than that for *Plasmodium* HDAC (Chua *et al.*, 2017).

Many studies have reported the effect of HDAC inhibitors on *P. falciparum* (Andrews *et al.*, 2012; Engel *et al.*, 2015; Chua *et al.*,

https://doi.org/10.1017/S0031182022000427 Published online by Cambridge University Press

2017). However, very little is known about other apicomplexan parasites of medical interest, such as *T. gondii* and *C. parvum*. We have hereby modelled and provided insights regarding these parasites' HDACs, discussing promising drugs for treating these diseases as well as potential residues to be targeted when considering drug development. We emphasize the importance of further studies, especially *in vivo*, to confirm the inhibitory potential of these compounds and promote a better understanding of the structure of these proteins.

Supplementary material. The supplementary material for this article can be found at https://doi.org/10.1017/S0031182022000427

Author contributions. C. M. S., S. C. N. and T. A. C. B. S. conceived and designed the study. C. M. S., M. S. I. F. and V. R. S. performed homology modelling, molecular docking and structural analysis of complex with coordination of T. A. C. B. S. I. V. B. conducted and analysed molecular docking simulations. C. M. S., S. C. N., M. S. I. F., I. V. B. and T. A. C. B. S. wrote the article. All authors reviewed the submitted version of the article.

Financial support. This research received funding from FIOCRUZ, Inova-Geração de conhecimento (Fiotec VPPCB-007-FIO-18-2-92), PROEP 442339/2019-4, PRONEX (Programa de Apoio a Núcleos de Excelência: Edital: PI 01/2018 – Acordo FA/CNPqFA 41.2018) and CAPES.

Conflict of interest. The authors declare there are no conflicts of interest.

Ethical Standards. Not applicable.

References

Abraham MJ, Murtola T, Schulz R, Páll S, Smith JC, Hess B and Lindahl E (2015) GROMACS: high performance molecular simulations through multi-level parallelism from laptops to supercomputers. *SoftwareX* **1–2**, 19–25.

Anandakrishnan R, Aguilar B and Onufriev AV (2012) H++ 3.0: automating pK prediction and the preparation of biomolecular structures for atomistic molecular modeling and simulations. *Nucleic Acids Research* **40**, W537–W541.

Anderson RJ, Weng Z, Campbell RK and Jiang X (2005) Main-chain conformational tendencies of amino acids. *Proteins* **60**, 679–689.

Andrews KT, Gupta AP, Tran TN, Fairlie DP, Gobert GN and Bozdech Z (2012) Comparative gene expression profiling of *P. falciparum* malaria parasites exposed to three different histone deacetylase inhibitors. *PLoS One* **7**, e31847.

Balaji S (2005) Discovery of the principal specific transcription factors of Apicomplexa and their implication for the evolution of the AP2-integrase DNA binding domains. *Nucleic Acids Research* **33**, 3994–4006.

Ballante F, Reddy DR, Zhou NJ and Marshall GL (2017) Structural insights of SmKDAC8 inhibitors: targeting *Schistosoma epigenetics* through a combined structure-based 3D QSAR, in vitro and synthesis strategy. *Bioorganic & Medicinal Chemistry* **25**, 2105–2132.

Benedetti R, Conte M and Altucci L (2015) Targeting histone deacetylases in diseases: where are we? *Antioxidants & Redox Signaling* **23**, 99–126.

Bougdour A, Maubon D, Baldacci P, Ortet P, Bastien O, Bouillon A, Barale J-C, Pelloux H, Ménard R and Hakimi M-A (2009) Drug inhibition of HDAC3 and epigenetic control of differentiation in Apicomplexa parasites. *The Journal of Experimental Medicine* **206**, 953–966.

Bussi G, Donadio D and Parrinello M (2007) Canonical sampling through velocity rescaling. *The Journal of Chemical Physics* **126**, 014101.

Chaal BK, Gupta AP, Wastuwidyaningtyas BD, Luah Y-H and Bozdech Z (2010) Histone deacetylases play a major role in the transcriptional regulation of the *Plasmodium falciparum* life cycle. *PLoS Pathogens* **6**, e1000737.

Chahal V, Nirwan S and Kakkar R (2020) Combined approach of homology modeling, molecular dynamics, and docking: computer-aided drug discovery. In Ramasami P (ed.), *Computational Chemistry Methods: Applications*, Vol. **4**. Berlin, Boston: De Gruyter, pp. 63–88. https://doi.org/10.1515/9783110631623-005.

Chua MJ, Arnold MSJ, Xu W, Lancelot J, Lamotte S, Späth GF, Prina E, Pierce RJ, Fairlie DP, Skinner-Adams TS and Andrews KT (2017) Effect of clinically approved HDAC inhibitors on *Plasmodium*, *Leishmania* and *Schistosoma* parasite growth. *International Journal for Parasitology: Drugs and Drug Resistance* **7**, 42–50.

Colletti SL, Myers RW, Darkin-Rattray SJ, Gurnett AM, Dulski PM, Galuska S, Allocco JJ, Ayer MB, Li C, Lim J, Crumley TM, Cannova C, Schmatz DM, Wyvratt MJ, Fisher MH and Meinke PT (2001) Broad spectrum antiprotozoal agents that inhibit histone deacetylase: structure–activity relationships of apicidin. Part 2. *Bioorganic & Medicinal Chemistry Letters* **11**, 113–117.

Darkin-Rattray SJ, Gurnett AM, Myers RW, Dulski PM, Crumley TM, Allocco JJ, Cannova C, Meinke PT, Colletti SL, Bednarek MA, Singh SB, Goetz MA, Dombrowski AW, Polishook JD and Schmatz DM (1996) Apicidin: a novel antiprotozoal agent that inhibits parasite histone deacetylase. *Proceedings of the National Academy of Sciences of the United States of America* **93**, 13143–13147.

Di Micco S, Terracciano S, Bruno I, Rodriquez M, Riccio R, Taddei M and Bifulco G (2008) Molecular modeling studies toward the structural optimization of new cyclopeptide-based HDAC inhibitors modeled on the natural product FR235222. *Bioorganic & Medicinal Chemistry* **16**, 8635–8642.

Dunay IR, Gajurel K, Dhakal R, Liesenfeld O and Montoya JG (2018) Treatment of toxoplasmosis: historical perspective, animal models, and current clinical practice. *Clinical Microbiology Reviews* **31**. doi: 10.1128/CMR.00057-17.

Engel JA, Jones AJ, Avery VM, Sumanadasa SDM, Ng SS, Fairlie DP, Skinner-Adams T and Andrews KT (2015) Profiling the anti-protozoal activity of anti-cancer HDAC inhibitors against *Plasmodium* and *Trypanosoma* parasites. *International Journal for Parasitology: Drugs and Drug Resistance* **5**, 117–126.

Essmann U, Perera L, Berkowitz ML, Darden T, Lee H and Pedersen LG (1995) A smooth particle mesh Ewald method. *The Journal of Chemical Physics* **103**, 8577–8593.

Frénal K, Dubremetz J-F, Lebrun M and Soldati-Favre D (2017) Gliding motility powers invasion and egress in Apicomplexa. *Nature Reviews. Microbiology* **15**, 645–660.

Guidi A, Saccoccia F, Gennari N, Gimmelli R, Nizi E, Lalli C, Paonessa G, Papoff G, Bresciani A and Ruberti G (2018) Identification of novel multistage histone deacetylase (HDAC) inhibitors that impair *Schistosoma mansoni* viability and egg production. *Parasites & Vectors* **11**, 668.

Haug EJ, Arora JS and Matsui K (1976) A steepest-descent method for optimization of mechanical systems. *Journal of Optimization Theory and Applications* **19**, 401–424.

Huang J, Rauscher S, Nawrocki G, Ran T, Feig M, de Groot BL, Grubmüller H and Grubmüller AD, Jr. (2017) HARMM36m: An improved force field for folded and intrinsically disordered proteins. *Nature Methods* **14**, 71–73.

Inoue A and Fujimoto D (1969) Enzymatic deacetylation of histone. *Biochemical and Biophysical Research Communications* **36**, 146–150.

Iwanaga S, Kaneko I, Kato T and Yuda M (2012) Identification of an AP2-family protein that is critical for malaria liver stage development. *PLoS One* **7**, e47557.

Jeninga M, Quinn J and Petter M (2019) ApiAP2 transcription factors in apicomplexan parasites. *Pathogens (Basel, Switzerland)* **8**, 47.

Jorgensen WL, Chandrasekhar J, Madura JD, Impey RW and Klein ML (1983) Comparison of simple potential functions for simulating liquid water. *The Journal of Chemical Physics* **79**, 926–935.

Joshi MB, Lin DT, Chiang PH, Goldman ND, Fujioka H, Aikawa M and Syin C (1999) Molecular cloning and nuclear localization of a histone deacetylase homologue in *Plasmodium falciparum*. *Molecular and Biochemical Parasitology* **99**, 11–19.

Kumar A, Dhar SK and Subbarao N (2018). In silico identification of inhibitors against *Plasmodium falciparum* histone deacetylase 1 (PfHDAC-1). *Journal of Molecular Modeling* **24**, 232.

Laskowski RA, Jabłońska J, Pravda L, Vařeková RS and Thornton JM (2018) PDBsum: structural summaries of PDB entries. *Protein Science* **27**, 129–134.

Lee J-H, Bollschweiler D, Schäfer T and Huber R (2021) Structural basis for the regulation of nucleosome recognition and HDAC activity by histone deacetylase assemblies. *Science Advances* **7**, eabd4413.

Melesina J, Robaa D, Pierce RJ, Romier C and Sippl W (2015) Homology modeling of parasite histone deacetylases to guide the structure-based design of selective inhibitors. *Journal of Molecular Graphics & Modelling* **62**, 342–361.

Miller TA, Witter DJ and Belvedere S (2003) Histone deacetylase inhibitors. *Journal of Medicinal Chemistry* **46**, 5097–5116.

Mori H, Urano Y, Abe F, Furukawa S, Furukawa S, Tsurumi Y, Sakamoto K, Hashimoto M, Takase S, Hino M and Fujii T (2003) FR235222, a

fungal metabolite, is a novel immunosuppressant that inhibits mammalian histone deacetylase (HDAC). I. Taxonomy, fermentation, isolation and biological activities. *The Journal of Antibiotics* **56**, 72–79.

Morrison DA (2009) Evolution of the Apicomplexa: where are we now? *Trends in Parasitology* **25**, 375–382.

Nardelli SC, Che F-Y, de Monerri S, Xiao NC, Nieves H, Madrid-Aliste E, Angel C, Sullivan SO, Angeletti WJ, Kim RH, and Weiss K and M L (2013) The histone code of *Toxoplasma gondii* comprises conserved and unique posttranslational modifications. *mBio* **4**. doi: 10.1128/mBio.00922-13.

Oberstaller J, Pumpalova Y, Schieler A, Llinás M and Kissinger JC (2014) The *Cryptosporidium parvum* ApiAP2 gene family: insights into the evolution of apicomplexan AP2 regulatory systems. *Nucleic Acids Research* **42**, 8271–8284.

Painter HJ, Campbell TL and Llinás M (2011) The apicomplexan AP2 family: integral factors regulating *Plasmodium* development. *Molecular and Biochemical Parasitology* **176**, 1–7.

Pettersen EF, Goddard TD, Huang CC, Couch GS, Greenblatt DM, Meng EC and Ferrin TE (2004) UCSF Chimera – a visualization system for exploratory research and analysis. *Journal of Computational Chemistry* **25**, 1605–1612.

Radke JR, Behnke MS, Mackey AJ, Radke JB, Roos DS and White MW (2005) The transcriptome of *Toxoplasma gondii*. *BMC Biology* **3**, 26.

Ramaprasad A, Mourier T, Naeem R, Malas TB, Moussa E, Panigrahi A, Vermont SJ, Otto TD, Wastling J and Pain A (2015) Comprehensive evaluation of *Toxoplasma gondii* VEG and *Neospora caninum* LIV genomes with tachyzoite stage transcriptome and proteome defines novel transcript features. *PLoS One* **10**, e0124473.

Sánchez R and Sali A (1997) Advances in comparative protein-structure modelling. *Current Opinion in Structural Biology* **7**, 206–214.

Sepehri Z, Beacon TH, Osman FDS, Jahan S and Davie JR (2019) DNA methylation and chromatin modifications. In *Nutritional Epigenomics*. United States: Elsevier, pp. 13–36. doi: 10.1016/B978-0-12-816843-1.00002-3.

Seto E and Yoshida M (2014) Erasers of histone acetylation: the histone deacetylase enzymes. *Cold Spring Harbor Perspectives in Biology* **6**, a018713.

Sippl MJ (1993) Recognition of errors in three-dimensional structures of proteins. *Proteins* **17**, 355–362.

Söding J, Biegert A and Lupas AN (2005) The HHpred interactive server for protein homology detection and structure prediction. *Nucleic Acids Research* **33**, W244–W248.

Srivastava S, White MW and Sullivan WJ (2020) *Toxoplasma gondii* AP2XII-2 contributes to proper progression through S-phase of the cell cycle. *mSphere* **5**. doi: 10.1128/mSphere.00542-20.

Terui Y, Chu Y, Li J, Ando T, Fukunaga T, Aoki T and Toda Y (2008) New cyclic tetrapeptides from *Nonomuraea* sp. TA-0426 that inhibit glycine transporter type 1 (GlyT1). *Bioorganic & Medicinal Chemistry Letters* **18**, 6321–6323.

Trott O and Olson AJ (2010) AutoDock Vina: improving the speed and accuracy of docking with a new scoring function, efficient optimization, and multithreading. *Journal of Computational Chemistry* **31**, 455–461.

Vaca HR, Celentano AM, Toscanini MA, Heimburg T, Ghazy E, Zeyen P, Hauser A-T, Oliveira G, Elissondo MC, Jung M, Sippl W, Camicia F and Rosenzvit MC (2021) The potential for histone deacetylase (HDAC) inhibitors as cestocidal drugs. *PLoS Neglected Tropical Diseases* **15**, e0009226.

Verdin E and Ott M (2015) 50 years of protein acetylation: from gene regulation to epigenetics, metabolism and beyond. *Nature Reviews. Molecular Cell Biology* **16**, 258–264.

Webb B and Sali A (2016) Comparative protein structure modeling using MODELLER. *Current Protocols in Bioinformatics* **54**, 5.6.1–5.6.37.

WHO Guidelines Approved by the Guidelines Review Committee (2015) *Guidelines for the Treatment of Malaria*, 3rd Edn, Geneva: World Health Organization.

Wiederstein M and Sippl MJ (2007) ProSA-web: interactive web service for the recognition of errors in three-dimensional structures of proteins. *Nucleic Acids Research* **35**, W407–W410.

https://doi.org/10.1017/S0031182022000427 Published online by Cambridge University Press